Original Article

Effect of Abrupt and Gradual withdrawal of Acrylamide on Acrylamide Induced Hepatic and Renal Cortical Injury of Adult Male Albino Rats: Histological and Immunohistochemical Study

Amira Fathy Ahmed, Randa Ahmed Ibrahim, Azza Hussein Ali and Esraa Mohammed Khairy

Department of Histology and Cell Biology, Faculty of Medicine, El-Minia University, Egypt

ABSTRACT

Introduction: Acrylamide (AA) became an urgent public health interest as it is commonly consumed in fast food cooked at high temperatures. Various health organizations recommend stoppage of its use in certain food due to its health hazards.

Aim of the Work: To investigate the effect of abrupt and gradual withdrawal of acrylamide on its destructive impact on the hepatic and renal cortical tissues.

Materials and Methods: Rats were classified into 4 groups 10 rats in every group. The control group (group I). The acrylamide group (group II): Acrylamide was orally administered at the dose of 20 mg/kg/day for 3 weeks. The abrupt withdrawal group (group III): Acrylamide was given by the same route as group II for 3 weeks, then abruptly stopped in the following 3 weeks. The gradual withdrawal group (group IV): Acrylamide was given by the same route as group II for 3 weeks then the acrylamide was gradually withdrawn in the following three weeks. Liver and renal cortical tissues were taken and used for histological (H&E, PAS and Masson stain), immunohistochemical (PCNA, caspase 3 and alpha SMA) and morphometric studies.

Results: The histological examination of the liver and renal cortical tissue section of groups II and IV revealed marked destruction of their architecture. On the other hand, group III showed marked improvement.

Conclusion: The usage of AA caused deleterious effects in liver and renal cortical tissues mainly due to reactive oxygen species (ROS) production. Stopping AA administration showed marked improvement in the histology of liver and renal tissue if compare with the its gradual withdrawal.

Received: 18 February 2022, **Accepted:** 20 March 2022

Key Words: AA (Acrylamide), ROS, withdrawal.

Corresponding Author: Amira Fathy Ahmed, MD, Department of Histology and Cell Biology, Faculty of Medicine, El-Minia University, Egypt, **Tel.**: +20 11 2276 0040, **E-mail:** amirafathy332@gmail.com

ISSN: 1110-0559, Vol. 46, No. 2

INTRODUCTION

Acrylamide (AA) is a substance which has an urgent public health importance as it is present in commonly used in bread, potato chips, and any carbohydrate-rich food items cooked at temperatures more than 200°C. AA is released during the roasting of coffee beans[1]. AA is used in synthesis of body lotions, cosmetics and other personal care products. In addition, it is also detected in tobacco smoke[2]. It is used in wastewater treatment, soil conditioning, pesticides and herbicides production[3].

AA is transmitted into the body via the following routes: digestive system, respiratory system, and skin absorption[4]. The Maillard reaction is one of main mechanisms of acrylamide generation process in foods and drinks[1]. Asparagine is a free amino acid which is needed to produce acrylamide. Asparagine and reducing sugars enter a reaction that is resulted in production of a decarboxylated Schiff base as precursor to AA[5]. Ammonia that is present in a high lipid amount food has also an important role to produce AA[6].

Production of AA in foods is mainly due to Maillard reaction, which is the first method that can be manipulated to reduce AA formation such as reducing time and temperature. High exposure to AA leads to many toxic effects, so it is necessary, especially in the developing countries to raise the awareness about AA health risks[1].

Many studies reported that AA has deleterious effects on liver, kidney, reproductive system, nervous system, DNA, and even cancer because of its continuous consumption[7]. Various health organizations recommend measuring its amount in certain food products[8].

Liver and kidneys are the organs concerned with elimination of half the amount of the AA daily dose[9]. Many studies assessed the effects of AA on the histological structure of liver and kidney. So, it is a must to stop the use of AA in many products that are used in our daily life. The main aim of our study to monitor and compare the sudden and gradual withdrawal effects of AA in reducing its damaging hazards on liver and renal cortices. These effects were assessed by histological, histochemical, immunohistochemical and morphometrical studies.

 DOI: 10.21608/ejh.2022.115268.1634

Animals

Forty adult male albino rats were used, weighing about 150-250 g aged about 6-8 weeks. Rats were got from the Animals Growing Center of the Faculty of Agriculture-Minia University. All rules of animal care and treatment were done regarding the guidelines of the Ethical Committee of the Faculty of Medicine-Minia University.

Experimental design and reagents

The 40 adult male albino rats were randomly classified into 4 groups (n=10 per group) as follows: Group I (Control group): They received distilled water and a standard diet for six-week ad libitum. Group II (Acrylamide group): They received Acrylamide, >99.5% purity with catalog no. 004027 bought from Medico company, Egypt. It was dissolved in 0.2 ml of distilled water and orally administered via intra-gastric gavage route at a dose of 20 mg/kg[10] once daily for three weeks[11]. Group III (Sudden withdrawal group): As group II but AA was given for three weeks then abruptly stopped in the next three weeks. Group IV (Gradual withdrawal group): As group II AA was given for three weeks then AA was gradually withdrawn with the same dose in the following three weeks, as follow: The fourth week: It was given three times per week. The fifth week: It was given two times per week. The sixth week: It was given once per week.

For light microscopic examination

At the end of expirement (3 weeks for group II and 6 weeks for groups I,III and IV), liver and kidney tissue sections from all groups were fixed in 10% formalin, embedded in paraffin and dehydrated in ascending concentrations of ethyl alcohol. 5 µm tissue sections were stained with hematoxylin and eosin (H&E), Periodic acid Schiff (PAS) to demonstrate general carbohydrates, and Masson trichrome stain for collagen deposition[12].

Immunohistochemical study

Immunocytochemical staining was performed according the manufacture instructions using the Anti-PCNA antibody for cell regeneration (anti-proliferating cell nuclear antigen): it is monoclonal mouse antibodies with catalog no. MA5-11358" from Thermo fisher Company, USA. Activated anti-caspase 3 antibodies for apoptosis: it is polyclonal rabbit antibodies with catalog no. PA1-26426" obtained from Thermo fisher Company, USA and Anti-alpha smooth muscle actin (alpha-SMA) antibody for myofibroblast identification: "mouse monoclonal antibody, catalog no. MA1-06110" obtained from Thermo fisher Company, USA.

4µm sections were cut for immune-labeling. The procedure was performed regarding the manufacture instructions. Briefly, sections were deparaffinized in xylene then rehydrated in descending concentrations of alcohol. After that, they were immersed in 0.1% hydrogen peroxide for 15 minutes to prevent the endogenous peroxidase activity. For antigen retrieval, the slides were boiled in 10mm citrate buffer solution (PH 6) for 10-20 min followed by cooling at room temperature for 20 min. Sections were washed by phosphate buffer then incubated in the ultra-vision block at room temperature for 5 minutes to prevent the non-specific background staining. Anti-PCNA, cleaved (activated) anti-caspase 3, and anti-alpha SMA antibodies were ready to be used. Sections were incubated with anti-PCNA antibody and anti-alpha SMA antibody for 60 minutes at room temperature. They were incubated for 15 minutes with the activated anti- caspase 3 antibodies at room temperature. After washing in a buffer, sections were incubated with biotinylated goat anti-rabbit secondary antibodies (1:1000) for 30 minutes before being washed. The reaction was seen with the usage of ultra-vision one detection System, HRP Polymer & (diaminiobenzide) DAB Chromogen (Thermo Fisher Company, USA). After fulfillment of the reaction, counterstaining was performed with the usage of Meyer's hematoxylin and dehydrated by exposure to ascending grades of alcohol then cleared by xylene. Coverslip using permanent mounting media was put. In negative control slides, the same system was performed except the primary antibodies were not added.

Photography

Olympus light microscopy (Olympus, Japan), at the Histology and Cell Biology Department at Faculty of Medicine, Minia University, was used for examination of the slides and capturing images for the sections. Images were saved as jpg form.

Morphometric analysis

At the faculty of Dentistry, Minia University, Image J 22 was used for measuring the area fraction of the activated caspase 3[13] and alpha-SMA immunopositivity[14]. Area fraction was measured in a standard measuring frame per 10 images in each group using a magnification X 400 by light microscopy. Areas containing positively immuno-stained tissues were used for estimation independent on the intensity of staining.

Measuring the mean number of PCNA immuno-positive cells

It was assessed by counting 10 non-overlapping fields using ×400 magnification in for the same slide of each animal[15].

Statistical analysis

SPSS (version 20, Windows 7, Office 2010) was used for statistical analysis of the collected numerical data. The mean and standard deviation (SD) were calculated for every group and the significance of differences detected was pooled and assessed by a one-way ANOVA test for quantitative data between the all groups. It is followed by post hoc Tukey analysis between every two groups. Significance was assessed according to the probability factor (*P-value*) $P<0.05$.

RESULTS

Histological study

Histological study for liver and kidney using hematoxylin and eosin

As regard liver tissue sections, the control group exhibited normal lobular architecture, with radiated plates of hepatocytes. The hepatocytes appeared polyhedral with acidophilic granular cytoplasm and rounded central vesicular nuclei and prominent nucleoli. They are radiating from the central veins forming anastomosing fenestrated plates separated by blood sinusoids that lined by endothelium with flat nuclei and Von Kupffer cells. Many binucleated hepatocytes were observed (Figure 1A). Examination of group II showed disrupted lobular architecture and marked hepatic injury. Central vein and hepatic sinusoids appeared congested and engorged with inflammatory cells. Ballooned hepatocytes with foamy vacuolated cytoplasm and malformed nuclei were observed. Some hepatocytes showed apoptotic features in the form of deep acidophilic cytoplasm and pyknotic nuclei. Inflammatory cells infiltration was seen between the hepatic tissue (Figure 1B). The group III exhibited marked morphological restoration, as there was preserved general hepatic architecture with hepatocytes restored their cytoplasm and most nuclei appeared normal and vesicular. However, scattered degenerated cells were still present. Vascular congestion was markedly reduced. Mild sinusoidal dilatation and few inflammatory cells infiltration could be seen (Figure 1C). Group VI showed more or less similar to group II beside markedly congested and engorged central vein with numerous inflammatory cells and hemosiderin laden macrophages (Figure 1D)

Examination of renal cortical tissue sections: the control group exhibited normal organization of the renal cortex consisting of renal corpuscles, proximal convoluted tubules (PCTs), and distal convoluted tubules (DCTs). Each renal corpuscle consists of glomerulus (a tuft of blood capillaries) surrounded by Bowman's capsule, with a urinary space in between. Bowman's capsule has an outer parietal layer consists of simple squamous epithelium, and an inner visceral layer forming the podocytes. The PCTs are lined by cubical cells with acidophilic cytoplasm. The DCTs have lower cubical epithelium surrounding relatively larger regular lumens (Figure 1a). Examination of group II sections showed distorted renal corpuscle with shrunken and congested glomerular tufts with widening of the Bowman's space. Renal tubular lining cells showed abundant cytoplasmic vacuolations, malformed nuclei and tubular distortion. Tubular lumina exhibited pyknotic nuclei, cellular debris or hyaline casts. Sever interstitial hemorrhage with hemosiderin laden macrophages and numerous inflammatory cells were observed. Numerous interstitial fibroblasts were noticed (Figure 1b). Abrupt withdrawal of acrylamide in group III ameliorated its damaging effects. There was restoration of normal cortical structure, with well-formed glomerular tuft and Bowman's space. Most PCTs and DCTs apparently retained their normal structure. Few tubules showed signs of degeneration in their lining cells and minimal intraluminal cellular debris (Figure 1c). While gradual withdrawal of acrylamide in group IV revealed no improvement compared to group II. There was marked distortion of the renal cortex in the form of hypertrophied renal corpuscle with congested glomerular tuft and widening of the Bowman's space. Renal tubules showed degenerated lining cells. Sever interstitial vascular congestion and dilatation with hemosiderin laden macrophages and inflammatory cells infiltration. Numerous interstitial fibroblasts and peritubular homogenous acidophilic material were seen (Figure 1d).

Histological study for liver and kidney using PAS stain

Examination of rat liver tissue sections showed PAS positive carbohydrates in the cytoplasm of most hepatocytes in the control group (Figure 2A). There was marked decrease in the glycogen content in most hepatocytes in groups II and IV (Figures 2B, 2D). On the other hand, restored PAS positive carbohydrates in the cytoplasm of most hepatocytes in group III (Figure 2C)

Examination of rat renal cortical tissue sections of the control group revealed positive reaction in the basement membranes of the glomerular capillaries, parietal layer of Bowman's capsule, and in the renal tubules. Positive reaction in the brush border of PCTs was noticed (Figure 2a). Group II and IV revealed partial loss of basement membranes of glomerular capillaries, parietal layer of Bowman's capsule and renal tubules. Thickening of some areas of basement membranes of glomerular capillaries, parietal layer of Bowman's capsule and renal tubules. Loss of brush borders of PCTs (Figures 2b,2d). While group IV exhibited restored positive reaction in the basement membranes of the glomerular capillaries, parietal layer of Bowman's capsule and most of renal tubules. PCTs lining cells restored brush borders (Figure 2c).

Histological study for liver and kidney using Masson trichrome stain

Liver tissue sections of the control group showed minimal amount of collagen fibers in the portal area (Figure 3A). Groups II and IV revealed marked increase in the collagen deposition around the congested dilated blood vessels in the portal area (Figures 3B,3D). While in the group III, there was little amount of collagen fibers in the portal area (Figure 3C). Renal cortical tissue sections of the control group showed minimal amount of collagen fibers among the glomerular tuft and interstitial tissue (Figure 3a). Groups II and IV exhibited dense collagen deposition among the glomerular tuft and interstitial tissue (Figures 3b,3d). There was marked decrease in the collagen deposition among the glomerular tuft and interstitial tissue (Figure 3c).

Immunohistochemical study

Immunohistochemical study for liver and kidney using PCNA

Examination of wide fields of liver tissue sections of the control group showed scattered positive immunoreactive nuclei in hepatocytic cells (Figure 4A). In regard to group II, there were few hepatocytes with immunopositively nuclei. (Figure 4B). On the other hand, groups III and IV showed numerous cells with positive nuclear immunoreactivity (Figures 4C,4D). Examination of wide fields of renal cortical tissue of the control group showed scattered renal cells with positive immunoreactive nuclei (Figure 4a). Group II showed few immuno-positive glomerular cells and renal tubular cells (Figure 4b). Numerous immuno-positive glomerular cells and renal tubular cells were observed in groups III and IV (Figures 4c,4d).

Liver and renal cortex tissue sections showed significant increase in the mean number of PCNA immuno-positive cells in group II compared to control group. Significant increase in the mean number of PCNA immuno-positive cells in groups III and IV compared to control group and group II (Figure 4III).

Immunohistochemical study for liver and kidney using cleaved (activated) caspase -3

Examination of liver tissue sections of the control group showed no detectable activated caspase- 3 immunolabeled cells (Figure 5A). Extensive immunolabeling was markedly observed in the cytoplasm and nuclei of most hepatocytes in groups II and IV (Figures 5B,5D). Group III showed marked decrease in the expression compared to group II and IV (Figure 5C). Examination of renal cortical tissue sections of the control group showed no detectable activated caspase 3 immunolabeled cells (Figure 5a). Extensive immunolabeling was markedly observed in the cytoplasm and nuclei of most renal cells in groups II and IV (Figures 5b,5d). Group III showed marked decrease in the activated caspase 3 expression compared to group II and IV (Figure 5c).

Liver and renal cortex tissue sections showed significant increase in the area fraction of activated caspase 3 immuno-positive cells in groups II, III and IV compared to control group. Significant decrease in the area fraction of cleaved caspase 3 immuno-positive cells in group III compared to groups II and IV (Figure 5III).

Immunohistochemical study for liver and kidney using alpha smooth muscle actin

The control group exhibited positive expression in the wall of portal vein, hepatic artery and few faintly expressed cells stellate in shape with fine processes that extend between the hepatocytes in periportal area (Figure 6A). While groups II and IV (Figures 6B,6D) showed strong expression in walls of the portal vein and hepatic artery and numerous positive stellate cells between the hepatocytes in periportal area. Group III revealed positive reaction in the wall of portal vein, hepatic artery and few faintly expressed cells in-between hepatocytes (Figure 6C).

Positive expression in wall of renal blood vessels was observed in groups I (Figures 6a,b,c,d). Positive reaction in the renal glomerulus and the interstitial cells was obvious in groups II and IV (Figures 6b,6d). Faint expression in few renal glomerular cells and in few interstitial cells was observed in group III (Figure 6c).

Liver and renal cortex tissue sections showed significant increase in the area of fraction alpha smooth muscle actin in groups II, III and IV compared to group I. Significant decrease in the mean area fraction of alpha smooth muscle actin immuno-positive cells in group III compared to groups II and IV (Figure 6III).

Figure 1I

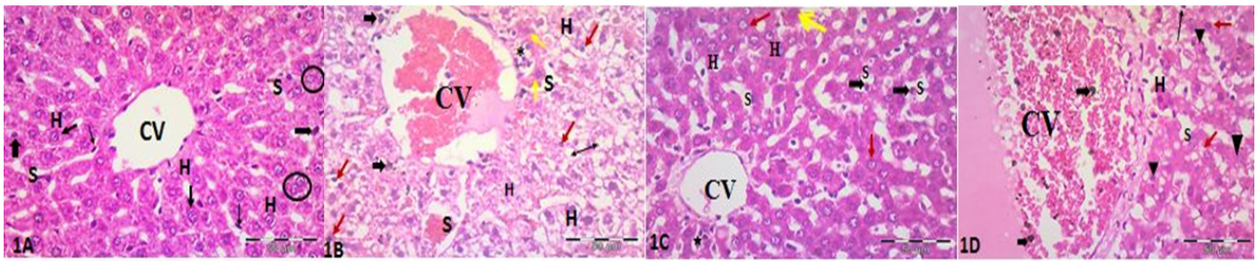

Figure 1 II

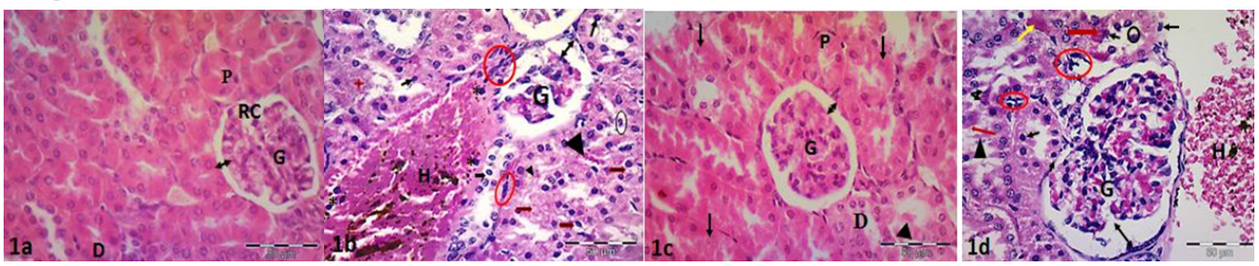

Fig.1 I: Representative photomicrographs of rat liver tissue showing the hepatocytes(H) are radiating from the central veins (CV) and separated by blood sinusoids (S). 1A) Control group showing the lobular architecture consist of plates of polygonal hepatocytes with an acidophilic granular cytoplasm and rounded vesicular nuclei with prominent nucleoli (black arrows) other cells appeared binucleated (circle). Notice the blood sinusoids are lined by endothelium with flat nuclei (thin arrows) and Von Kupffer cells (thick arrows). 1B) Acrylamid group showing loss of lobular architecture and sever congestion of central vein. It is surrounded by ballooned hepatocytes with foamy vacuolated cytoplasm and deformed dense nuclei (red arrows) or devoid of nuclei (double head arrow). Other hepatocytes have deep acidophilic cytoplasm and dense nuclei (yellow arrows). Sinusoidal congestion and dilatation around central vein are also seen. Note the presence of Von Kupffer cells (thick arrows) and mononuclear inflammatory cells infiltration; mainly lymphocytes (star) between degenerated hepatocytes. 1C) Abrupt withdrawal group showing restored lobular architecture. Apparent normal hepatocytes arranged in cords (red arrows) surrounding the central vein. Few degenerated hepatocytes with strong acidophilic cytoplasm and fading nuclei (yellow arrow). Notice mild sinusoidal dilatation with Von Kupffer cells (thick arrows) and some mononuclear inflammatory cells (star). 1D) Gradual withdrawal group showing loss of lobular architecture and massive congestion of central vein with numerous hemosiderin laden macrophages (thick arrows). Central vein surrounded with many degenerated hepatocytes with vacuolated cytoplasm (red arrows) and ghosts of nuclei (head arrows). Sinusoidal dilatation and mononuclear inflammatory cells infiltration are seen between degenerated hepatocytes (thin arrow).

Fig.1 II: Representative photomicrographs of rat renal cortex showing renal corpuscles (RC) formed glomerular tuft (G) and urinary space (double head arrow). It is surrounded by proximal convoluted tubule PCTs (P), and distal convoluted tubules DCTs (D). 1a) Control group showing normal lobular organization of the renal cortex consisting of renal corpuscles, PCTs, and DCTs. Notice the urinary space around the glomerular tuft & the regular distinct lumina of convoluted tubules. 1b) Acrylamid group showing distorted renal corpuscle with shrunken and congested glomerular tufts with widening of the urinary space. Some tubular lining cells appear with vacuolated cytoplasm, and others with disappearance of cytoplasm (red arrows). Some tubular cells have dense nuclei (black arrows), while others are devoid of nuclei (+). Some tubules show pyknotic nuclei (black circle), cellular debris and hyaline casts (head arrow) in their lumen. Sever interstitial hemorrhage with hemosiderin laden macrophages (H) and many mononuclear inflammatory cells (*) are also seen. Notice presence of numerous interstitial fibroblasts (red circles). 1c) Abrupt withdrawal group showing well-formed glomerular tuft (G) and Bowman's space. Most PCTs and DCTs are lined with apparently normal tubular cells. Few tubular cells with vacuolated cytoplasm and ghosts of nuclei (black arrows). Notice minimal intraluminal cellular debris (head arrow).1d) gradual withdrawal group showing hypertrophied renal corpuscle with congested glomerular tuft and widening of the urinary space. Some tubular lining cells with vacuolated cytoplasm and others with strong acidophilic cytoplasm (red arrows) are present. Some tubular cells with dense nuclei (black arrows) others fragmented nuclei (double arrows). Some tubules show pyknotic nuclei (black circle) and cellular debris (head arrow) in their lumen. Sever interstitial vascular congestion and dilatation with hemosiderin laden macrophages (H). Notice presence of numerous interstitial fibroblasts (red circles) and peritubular homogenous acidophilic material (Yellow arrow). (H&E x 400, scale bar= 50µm)

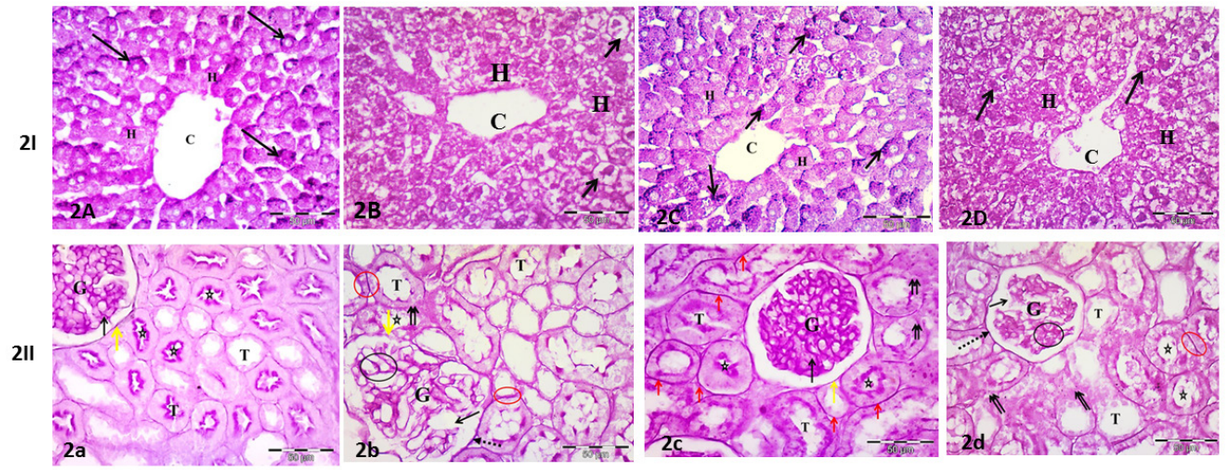

Fig. 2: I: Representative photomicrographs of rat liver tissue sections stained by PAS, showing the hepatocytes(H), with positive (magenta red) cytoplasmic total carbohydrates (black arrows) radiating from the central veins (C). 2A) control group showing positive PAS reaction in most hepatocytes. 2B) Acrylamid group with marked decrease in the carbohydrates in most hepatocytes. 2C) Abrupt withdrawal group with restored positive PAS reaction of most hepatocytes. 2D) Gradual withdrawal group with few carbohydrates in most hepatocytes.

Fig. 2: II: Representative photomicrographs of rat cortical renal tissue sections stained by PAS showing positive reaction (magenta red) in the basement membranes (black arrow) of the glomerular capillaries (G), parietal layer of Bowman's capsule (yellow arrow) and renal tubules (T). 2a) control group with positive reaction in the basement membranes of the glomerular capillaries, parietal layer of Bowman's capsule and renal tubules. Notice a strong positive reaction in the brush border of Proximal convoluted tubules (black stars). 2b) Acrylamid group showing partial loss of basement membranes (black arrow) of glomerular capillaries, parietal layer of Bowman's capsule (yellow arrow) and renal tubules (double arrows). Thickening of some areas of the basement membranes of glomerular capillaries (black circle), parietal layer of Bowman's capsule (dotted arrow) and renal tubules (red circles). Loss of brush borders of Proximal convoluted tubules (black stars). 2c) Abrupt withdrawal group showing continuous basement membranes (black arrow) of the glomerular capillaries and the parietal layer of Bowman's capsule. Most renal tubules show intact basement membranes (red arrows) while few tubules lose their basement membranes (double arrows). Notice Proximal convoluted tubules lining cells show preserved brush borders (black stars). 2d) Gradual withdrawal groupshowing partial loss of basement membranes (black arrow) of glomerular capillaries and renal tubules (double arrows). Thickening of some areas of basement membranes of glomerular capillaries (black circle), parietal layer of Bowman's capsule (dotted arrow) and renal tubules (red circle). Notice loss of brush borders of Proximal convoluted tubules (black stars). (PAS x 400, scale bar= 50µm).

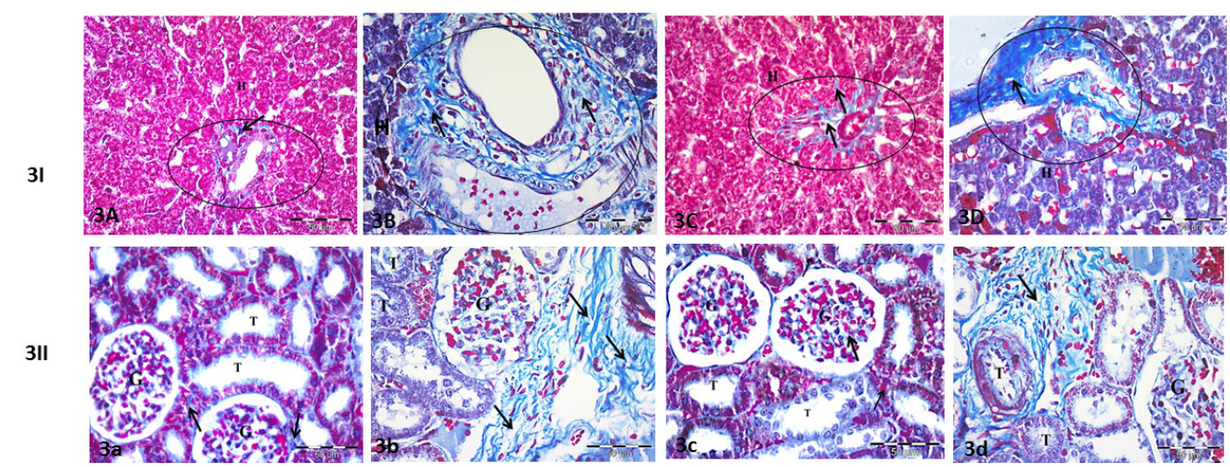

Fig. 3: I: Representative photomicrographs of rat liver tissue sections stained by Masson trichrome showing the hepatocytes (H) and portal area (black circle). Notice collagen fibers appear with blue color (black arrows). 3A) control group: showing minimal collagen deposition in the portal area. 3B) Acrylamid group showing dense collagen deposition around the congested dilated blood vessels in the portal area. 3C) Abrupt withdrawal group showing mild collagen deposition in the portal area. 3D) Gradual withdrawal group showing collagen deposition around the dilated blood vessels in the portal area.

Fig. 3: II: Representative photomicrographs of rat renal cortical tissue stained by Masson trichrome showing collagen fibers (blue color) among the glomerular tuft (G), tubules (T), and interstitial tissue (black arrows): 3a) Control group showing minimal amount of collagen fibers among the glomerular tuft and interstitial tissue. 3b) Acrylamid group showing dense collagen deposition among the glomerular tuft and interstitial tissue. 3c) Abrupt withdrawal group showing little amount of collagen fibers among the glomerular tuft and interstitial tissue. 3d) Gradual withdrawal group showing dense collagen fibers deposition among the glomerular tuft and interstitial tissue. (Masson trichrome x 400, scale bar= 50µm).

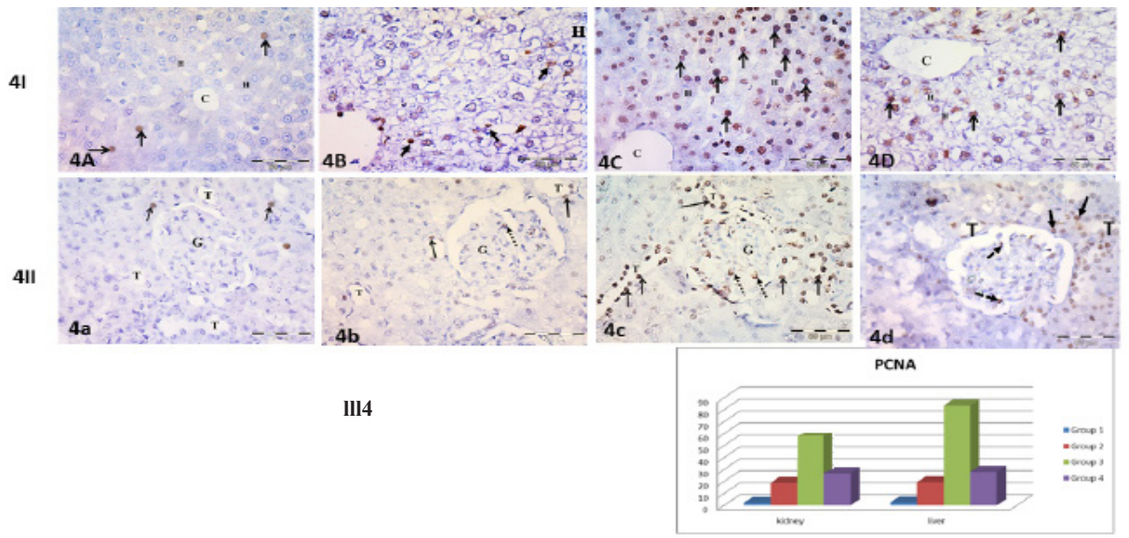

Fig. 4: I: Representative photomicrographs of rat liver tissue sections immunohistochemical stained for PCNA showing central vein (C) surrounded by cords of hepatocytes (H). Notice the positive immunoreactive nuclei in the cells (black arrows). 4A: Control group showing scattered positive immunoreactive nuclei in hepatocytic cells. 4B: Acrylamide group showing positive immunoreactive nuclei in few hepatocytic cells. 4C) Abrupt withdrawal group showing numerous hepatocytes have positive immunoreactivity in their nuclei. 4D) Gradual withdrawal group showing positive immunoreactive nuclei in many hepatocytic cells.
Fig. 4: II: Representative photomicrographs of rat renal cortical tissue immunohistochemical stained for PCNA showing renal glomeruli (G) and renal tubules (T) positive immunoreactive nuclei of (black arrows): 4a) Control group showing scattered renal positive tubular cells. 4b) Acrylamid group showing few positive immunoreactive nuclei of renal glomerular cells (dotted arrow) and renal tubular cells. 4c) Abrupt withdrawal group showing numerous positive immunoreactive nuclei of renal glomerular cells (dotted arrows) and renal tubular cells. 4d) Gradual withdrawal group with few positive immunoreactive nuclei of renal glomerular cells (dotted arrow) and renal tubular cells. Notice. III: The mean number of PCNA immunopositive nuclei among the four groups. (PCNA x 400, scale bar= 50µm).
Fig. 4: III4: The mean number of PCNA immunopositive cells among the four groups

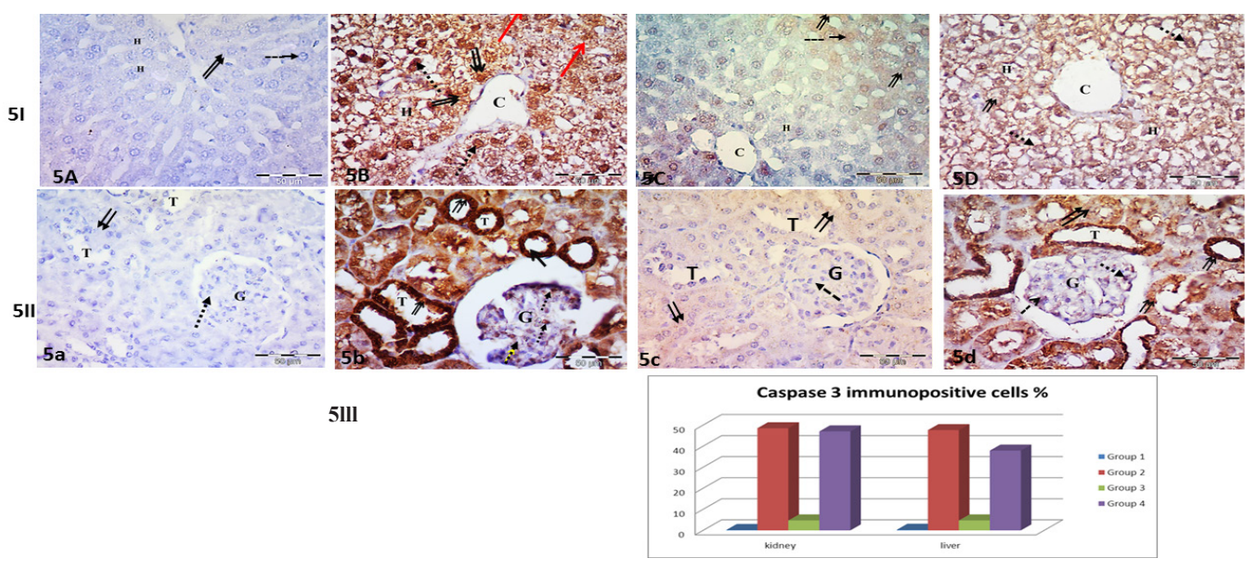

Fig. 5: I: Representative photomicrographs of rat liver tissue sections immunohistochemical stained for caspase 3 showing central vein (C) surrounded by cords of hepatocytes (H). Notice positive immunoreactivity in cytoplasm (double arrows) and nuclei of the cells (dotted arrows) :5A: The control group showing negative immunoreactivity in cytoplasm of hepatocytes. 5B) Acrylamid group showing strong positive immunoreactivity in cytoplasm and nuclei of most hepatocytes (H). 5C) Abrupt withdrawal group showing faint immunoreactivity in cytoplasm and nuclei of most hepatocytes. 5D) Gradual withdrawal group showing strong positive immunoreactivity in cytoplasm and nuclei of hepatocytes.
Fig. 5: II: Representative photomicrographs of rat renal cortical tissue immunohistochemical stained for caspase 3 showing renal glomerular cells (G) (dotted arrows) renal tubular lining cells (T) (double Arrow):5a) Control group: showing negative immunoreactivity in cytoplasm and nuclei of renal glomerular cells and renal tubular cells. 5b) Acrylamid group showing strong positive immunoreactivity in cytoplasm and nuclei of renal glomerular cells, and cytoplasm and nuclei of renal tubular cells. 5c) Abrupt withdrawal group showing faint expression in cytoplasm and nuclei of the renal glomerular cells and renal tubular cells. 5d) Gradual withdrawal group showing strong positive immunoreactivity in cytoplasm and nuclei of the renal glomerular cells, cytoplasm and nuclei of renal tubular lining cells. III: The area fraction of caspase 3 immunoreactivity among the four groups. (Caspase 3 x 400, scale bar= 50µm).
Fig. 5: 5III: The area fraction of activated caspase 3 immunopositive cells among the four groups

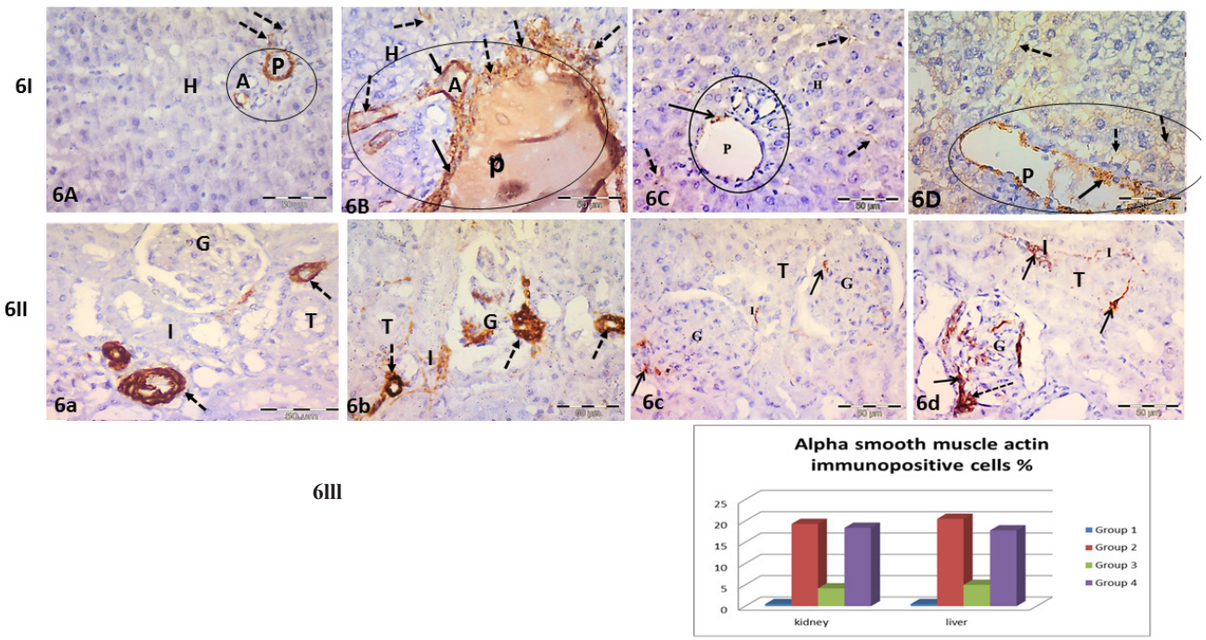

Fig. 6: I: Representative photomicrographs of rat liver tissue sections immunohistochemical for alpha smooth muscle actin showing: portal vein (P), hepatic artery (A) in the portal area (black circles) positive cells (black arrows) and hepatocytes (H). 6A) Control group showing positive expression in the wall of portal vein, hepatic artery and few faintly expressed cells stellate in shape with fine processes that extend between the hepatocytes in periportal area (dotted arrows). 6B) Acrylamid group showingstrong expression in the portal area in walls of the portal vein and hepatic artery and numerous positive stellate shaped cells fine processes that extend between the hepatocytes in periportal area (dotted arrows). 6C) Abrupt withdrawal group showing positive reaction in the wall of portal vein, hepatic artery in the portal area and few faintly expressed cells in-between hepatocytes. 6D) Gradual withdrawal group showing positive reaction in the wall of portal vein and numerous positive cells in-between hepatocytes (dotted arrows)

Fig. 6: II: Representative photomicrographs of rat renal cortical tissue sections immunohistochemical stained for alpha smooth muscle actin showing the wall of renal vessels (dotted arrows), the renal glomerulus (G) renal tubules (T), and the interstitial cells (I): 6a) Control group showing positive expression in vascular smooth muscles of renal blood vessels (arrows) and negative expression n glomeruli, renal tubules and interstitium. 6b) Acrylamid group showing positive immunoreactivity in the wall of renal vessels, in the renal glomerulus and the interstitial cells 6c) abrupt withdrawal group showing faint expression in few renal glomerular cells (black arrows) and in few interstitial cells. 6d) Gradual withdrawal group showing positive reaction in the wall of renal vessels (black arrows), in the renal glomerulus and in the interstitial cells. III: The area fraction of alpha smooth muscle actin immunopositive cells among the four groups. (Alpha smooth muscle actin antibody x400, scale bar =50 µm).

Fig. 6: 6III: The mean fraction of alpha smoth muscle actin immunopositive cells among the four groups

DISCUSSION

AA is a food contaminant used in a wide range in fast foods and in any carbohydrate-rich food cooked at high temperatures. It has toxic effects on human body but unfortunately it can't be easily avoided[1]. Exposure to AA occurs in other ways in our daily life such as materials of personal care and cosmetic products[16].

Furthermore, many researchers reported that AA can induce many health hazards[8]. Many studies were conducted to figure out the histological changes occur in hepatic and renal tissues after AA exposure and after use antioxidant agents for protection from its toxicity. On the other hand, there is no study comparing or evaluating the impact of the sudden and gradual withdrawal of AA on its induced hepatic and renal injuries.

Forty adult male albino rats were used in the work. Rats were divided into four groups, 10 animals in each group. Group I was the control group. Group II (acrylamide group) received acrylamide orally at a dose of 20 mg kg once daily for three weeks. Group III (sudden withdrawal group) received acrylamide orally at a dose of 20 mg/kg once daily for three weeks then acrylamide was abruptly stopped in the following three weeks. Group IV (gradual withdrawal group) received acrylamide orally at a dose of 20 mg/kg once daily for the first three weeks. In the following three weeks, acrylamide was withdrawn gradually.

In the present study, the acrylamide administration caused severe hepatic damage in groups II and IV, in the form of apoptosis, cytoplasmic vacuolations, inflammatory cells infiltration and vascular congestion and dilatation. Similar findings were were observed by Gedik S *et al*[17] who stated that AA administration caused many inflammatory cell infiltration, hepatocellular necrosis, areas of hemorrhage, loss of cellular boundaries and cytoplasmic vacuolations. This could be were observed by Gedik S *et al*[18] who reported that cytoplasmic vacuolations may be considered as a cellular defense mechanism against toxins because these vacuoles gather the harmful elements and prevent their harmful effect on the cellular activities. As well, free radicals attack polyunsaturated fatty acids of cell membranes leading to their degradation and formation

of cytoplasmic vacuoles. Kovac *et al* stated that AA causes a decrease in the reduced glutathione (GSH) which leads to mitochondrial dysfunction, reactive oxygen species (ROS) release, and oxidative stress harmful effects[19]. Moreover, this toxicity may cause damage to DNA and RNA, certain enzymes oxidative deactivation, and lipid peroxyl radical and lipid hydroxides liberation that cause imbalance between cell survival and death[10].

In this study, renal cortical sections of both group II&IV revealed also an inflammatory cellular infiltration and many tubular damages. The similar findings were observed by Jiang *et al* who reported that there were severe renal damages such as kidney tubule cavity widening, renal tubular cellular degeneration and interstitial inflammatory cell infiltration in the AA administered group[20]. El Fakahany *et al*., added several histopathological manifestations including deformed glomerular tuft with widened Bowman's space. The renal tubular cells became vacuolated and lost their brush border[21]. So, the degenerative changes could be observed in their epithelial lining followed by cellular rupture, apoptosis, vascular congestion of the interstitial tissue which led to hemorrhagic areas. There was accumulation of hyaline casts and proteinaceous materials in the lumen of the renal tubules.

The previous findings could be also explained by Erdemli *et al*., who stated that kidney has a major role in elimination of AA toxic substance in urine, moreover it has a weak antioxidant defense enzyme system so it is more vulnerable to be exposed to its toxic effect[22]. In our study, kidney tissue sections of the same group revealed cytoplasmic vacuolations of the tubular lining cells. Besides, ROS disturbed the vascular function leading to more cellular damage, apoptosis and inflammatory cells infiltration with vascular congestion and dilatation[23]. Raju *et al*., reported that AA decreased high-density lipoprotein (HDL) level which is associated with thickening, narrowing and blockage of the blood vessels leading to deleterious effect on them[24]. Elhelaly *et al*., stated that ROS produced by AA caused inflammation and dilatation of blood vessels to increase the blood flow to the injured area and this caused hemorrhage in the interstitium[10].

Sudden withdrawal of acrylamide in group III led to marked improvement in histological structure of both hepatic and renal tissues. At the level of liver tissue many hepatocytes were preserved with large vesicular nuclei. However, few hepatocytes still with pyknotic nuclei and vacuolated cytoplasm. On the other hand, kidney showed preserved histological architecture of a renal corpuscle and most of the renal tubules. This damage caused by AA occurred depending on its dose as the body can eliminate low AA doses through its detoxification. While mild and high doses caused degenerative changes and damage to different organs[25]. Besides, withdrawal of acrylamide caused restoration of the reduced glutathione and decrease in ROS production in sudden withdrawal of acrylamide[26].

In controversy to group III, group IV (gradual withdrawal group), there were apoptosis of hepatocytes and vascular congestion. Also, in kidney sections, there were apoptosis of glomerular and tubular lining cells and areas of inflammatory cellular infiltrations. The same was observed by Atef *et al*., who explained that low doses of AA exhibited normal renal cortex while high doses led to proliferative glomerulonephritis[26]. So, the chronic use of AA even with low doses led to accumulation of toxin and not give more time to tissues to come over it.

In regard to PAS stain, to assess glycogen production in liver tissue, the sections of groups II and IV, showed marked decrease in the glycogen granules in most hepatocytes if compare to control group. This also observed by Younes *et al*., who reported weak PAS positive reaction in most of liver cells treated with AA[27]. This observation could be explained that AA could produce extensive damage on hepatocytic integrity and function[19]. Moreover, reduced glycogen may be also due to intensive AA biotransformation instead of cellular metabolism[18].

In kidney sections of groups II and IV, there have been partial loss of the basement membranes of glomerular capillaries, the parietal layer of Bowman's capsule, basement membranes of renal tubules and loss of brush borders in many PCTs. That was also observed by Atef *et al*., who reported that PAS-stained sections of AA group within the renal tubules showed partially lost and weak PAS positive reaction in basement membranes renal tubules and PCT brush border[26]. These findings may be explained by the fact that ROS produced by AA which caused cellular atrophy and basement membrane damage[26].

In our study, the improvement was obviously noticed in group III and this could be explained that AA affects glycogen content depending on its administration dose[19]. Reckoning on this fact, our study suggested that the stoppage of AA exposure led to marked improvement within the function and structure of both hepatocyte and renal cortical tissue.

In regard to the extracellular matrix (ECM), Masson's trichrome stain was used to detect the role of acrylamide in induction of fibrosis. In the control liver, there was a minimal amount of collagen fibers in the portal tract. Groups II and IV exhibited marked increase in the amount of collagen fibers around the portal tract of liver tissue sections. It was reported that there was high collagen fibers deposition around the portal triad due to damage of stellate cells which are concerned with collagen fiber production[26]. It was explained that the occurrence and progression of fibrotic diseases were due to ROS and proinflammatory cytokines release including TNF and IL1β[28]. These cause hepatic stellate cells resist death thus formation of fibrous tissue[29]. Besides, the injured hepatocytes release aldehyde end products which cause further damage and fibrosis[30].

At the level of renal cortical tissue, groups II and IV in the present study exhibited marked increase in the collagen

fibers deposition in the glomerular tuft and interstitial tissue. It was observed that there was an increasing amount in collagen fiber deposition in between glomerular capillaries, however the renal tubules were still surrounded with few collagen fibers[26]. This is also due to oxidative stress and ROS generation. Renal fibrosis is the main pathway of progressive renal diseases which lead to end-stage renal failure regardless the cause. The development of fibrosis includes interstitial hyper cellularity, matrix accumulation, and epithelial cell atrophy, resulting in loss of normal function and organ failure[31].

In this study, immunohistochemically staining for PCNA was done to investigate renal and liver tissue regeneration. There was a significant increase in the mean number of PCNA positive nuclei in liver and kidney tissue sections of group III compared with groups II & IV. This was in agree with Lee *et al*., who reported that AA is an electrophile and reacts with macromolecules nucleophilic residues such as cellular proteins and their DNA leading to their damage. Besides, AA affects kinesin proteins that are responsible for the formation of spindle fibers during cell division and causing inhibition of cellular proliferation in groups II & IV[32].

As a marker of apoptosis activated caspase 3 was used. There was a significant decrease in the surface area fraction in liver and kidney tissue sections of group III compared with groups II and IV. This was explained that AA induces apoptosis in liver cells through the activation of both caspase-8 and-9[33]. It also causes defect in the activity of complex I and III of the mitochondrial electron transfer chain. Leading to promotion of the pro-apoptotic proteins activity which impair anti-apoptotic protein's function. This elicits the activity of the caspase cascade and induction of apoptosis[34].

As regard renal tissue, it was stated that in the normal cells, NF-kB is inactive in the cytoplasm due to binding to its inhibitors (p105, and IkBα-like protein[35]. In our study, AA exposure stimulated renal tubular cell apoptosis and significantly increased renal caspase-3 expression. This could be due to production of ROS and lipid peroxidation, and depletion of GSH that may lead to oxidative stress and destruction of NF-kB inhibitors. Its free dimers enter the nucleus and promote its anti-inflammatory genes and induction of cellular apoptosis. Furthermore, oxidative stress caused mitochondrial and lysosomal membranes damage and stimulate caspase-3 activation and consequently cell death[21].

In this work, immunohistochemical staining for alpha-SMA was done for the detection of myofibroblasts in liver and kidney tissues. There was a significant decrease in the surface area fraction of alpha-SMA immunoreaction in group III compared to group II and group IV in liver and renal tissue sections. While there was no significant difference between group II and group IV.

The previous results could be explained by Higashi *et al*., who mentioned that the presence of various triggering factors for hepatic stellate cells (HSCs) activation including; inflamed or injured hepatocytes microenvironment, ROS, hepatic toxins, apoptotic epithelial cells, and inflammatory mediators[36]. When hepatic stellate cells have been activated, they differentiated from lipid storing pericytes to myofibroblasts, which have contractile and proliferative ability. They are responsible for release of extracellular matrix molecules like collagen type I and collagen type III. Other quiescent fibro competent cellular elements as vascular tunica media smooth muscle cells, and fibroblasts in the Glisson's capsule can be transformed into myofibroblasts in response to liver damage[30].

While in liver tissue sections of group III, there were three mechanisms of improvement due to HSCs removal once injury subsides, the first one was apoptosis. The second mechanism was cellular senescence. It is a cell cycle arrest occurring when the cells exceed their proliferative capacity. The third mechanism was reversion (also known as 'deactivation') of activated stellate cells. The activated HSCs escaped from apoptosis during regression of liver fibrosis, underwent inhibition of fibro-genic genes, and acquired a phenotype the same as quiescent HSCs. These reverted HSCs still in quiescent state with its ability to become activated once exposed to fibro-genic stimuli[29].

At the extent of the renal tissue sections, in group II, in kidney tissue sections, there was a positive immunoreactivity within the interstitium and glomeruli. In kidney tissue sections of group III, marked improvement was observed. On the opposite hand, group IV showed minimal improvement this might be explained that the resident fibroblasts or pericytes differentiated in to αSMA-positive myofibroblasts in response to kidney damage[34].

From this study, it could be concluded that acrylamide exposure causes degenerative changes in the liver and kidney tissues in the form of cellular apoptosis, vacuolations, vascular congestion, and inflammatory cellular infiltration. Immunohistochemical and morphometric studies were performed for further evaluation of the effect of acrylamide administration and withdrawal changes. This damage is most likely due to ROS production and was more observed in the acrylamide group. We found in this study that sudden withdrawal of acrylamide causes marked improvement in the histology of the liver and kidney. On the other hand, gradual withdrawal caused minimal or no improvement if compared to the sudden withdrawal group.

RECOMMENDATIONS

It is highly recommended to eat healthy food rich in protective antioxidants instead of fast food and carbohydrate rich food cooked for long periods and at high temperature.

CONFLICT OF INTERESTS

There are no conflicts of interest.

REFERENCES

1. Rifai L and Saleh FA: A review on acrylamide in food: Occurrence, toxicity, and mitigation strategies. International journal of toxicology. (2020) 39(2), 93-102.
2. Abdullah SA: Toxicological Effects of Fried Potato Chips Supplementation on Young Rats. EC Nutrition. (2019) 14, 386-394.
3. Tepe, Y and Çebi A: Acrylamide in environmental water: a review on sources, exposure, and public health risks. Exposure and Health. (2019) 11(1), 3-12.
4. Vesper HW, Bernert JT, Ospina M, Meyers T, Ingham L, Smith A and Myers GL: Assessment of the relation between biomarkers for smoking and biomarkers for acrylamide exposure in humans. Cancer Epidemiology and Prevention Biomarkers. (2007) 16(11), 2471-2478.
5. Baskar G and Aiswarya R: Overview on mitigation of acrylamide in starchy fried and baked foods. Journal of the Science of Food and Agriculture. (2018) 98(12), 4385-4394.
6. Kuek SL, Tarmizi AH, Abd Razak RA, Jinap S, Norliza S and Sanny M: Contribution of lipid towards acrylamide formation during intermittent frying of French fries. Food Control. (2020) 118 (107), 430.
7. Rajeh NA: Acrylamide Toxicity and Mitigation Strategies: A Summary of Recent Reports. Journal of Pharmaceutical Research International. (2020), 154-163.
8. Abdel-Daim MM, El-Ela FIA, Alshahrani FK, Bin-Jumah M, Al-Zharani M, Almutairi B and Alkahtani S: Protective effects of thymoquinone against acrylamide-induced liver, kidney and brain oxidative damage in rats. Environmental Science and Pollution Research. (2020) 1-9.
9. Kandeil MA, Hassanin KM, Arafa MM, Abdulgawad HA and Safwat GM: Pomegranate peels ameliorate renal nitric oxide synthase, interleukin-1β, and kidney injury molecule-1 in nephrotoxicity induced by acrylamide in rats. Egyptian Pharmaceutical Journal. (2019)18(4), 368.
10. Elhelaly AE, AlBasher G, Alfarraj S, Almeer R, Bahbah EI, Fouda MM and Abdel-Daim MM: Protective effects of hesperidin and diosmin against acrylamide-induced liver, kidney, and brain oxidative damage in rats. Environmental Science and Pollution Research. (2020) 26(34), 35151-35162.
11. AL-Mosaibih MA: Effects of monosodium glutamate andacrylamide on the liver tissue of adult Wistar rats. Life Science Journal. (2013) 10(2): 35-42.
12. Suvarna KS, Layton C and Bancroft JD (Eds.): Bancroft's Theory and Practice of Histological Techniques E-Book, 8th ed. Elsevier Health Sciences. China. (2018) PP: 40-60, 153-175& 337-394.
13. Saber S, Mahmoud AA, Goda R, Helal NS, El-ahwany E and Abdelghany RH: Perindopril, fosinopril and losartan inhibited the progression of diethylnitrosamine-induced hepatocellular carcinoma in mice via the inactivation of nuclear transcription factor kappa-B. Toxicology letters. (2018) 295, 32-40.
14. Talele NP, Fradette J, Davies JE, Kapus A and Hinz B: Expression of α-smooth muscle actin determines the fate of mesenchymal stromal cells. Stem cell reports. (2015) 4(6), 1016-1030.
15. Srisowanna N, Choijookhuu N, Yano K, Batmunkh B, Ikenoue M, Mai NN and Hishikawa Y: The Effect of Estrogen on Hepatic Fat Accumulation during Early Phase of Liver Regeneration after Partial Hepatectomy in Rats. Acta histochemica et cytochemical. (2019) 52(4), 67-75.
16. Sharma K, Kaith BS, Kumar V, Som S, Kalia S and Swart HC: Synthesis and properties of poly (acrylamide-aniline) -grafted gum ghatti based nanospikes. RSC advances. (2014) 3(48), 25830–25839.
17. Gedik S, Erdemli ME, Gul M, Yigitcan B, Bag HG, Aksungur Z and Altinoz, E: Hepatoprotective effects of crocin on biochemical and histopathological alterations following acrylamide-induced liver injury in Wistar rats. Biomedicine & pharmacotherapy. (2017) 95, 764-770.
18. Ahrari Roodi P, Moosavi Z, Afkhami GA, Azizzadeh M and Hosseinzadeh H: Histopathological Study of Protective Effects of Honey on Subacute Toxicity of Acrylamide-Induced Tissue Lesions in Rats' Brain and Liver. Iranian Journal of Toxicology. (2018) 12(3), 1-8.
19. Kovac R, Rajkovic V, Koledin I and Matavulj M: Acrylamide alters glycogen content and enzyme activities in the liver of juvenile rat. Acta histochemical. (2015) 117(8), 712-717.
20. Jiang G, Lei A, Chen Y, Yu Q, Xie J, Yang Y and Su D: The protective effects of the Ganoderma atrum polysaccharide against acrylamide-induced inflammation and oxidative damage in rats. Food & Function. (2021) 12(1), 397-407.
21. El Fakahany GA, Nassar SA and Elballat SE: Alterations in Kidney of Albino Rat due to Acrylamide Exposure and the Possible Protective Role of l-arginine (Biochemical, Histological, Immunohistochemical and Molecular Study). Systematic Reviews in Pharmacy. (2021)12(3), 744-752.
22. Erdemli ME, Aksungur Z, Gul M, Yigitcan B, Bag HG, Altinoz E and Turkoz Y: The effects of acrylamide and vitamin E on kidneys in pregnancy: An experimental study. The Journal of Maternal-Fetal & Neonatal Medicine. (2019) 32(22), 3747-3756.

23. DeWitt DS and Prough DS: Blast-induced brain injury and posttraumatic hypotension and hypoxemia. Journal of neurotrauma. (2009) 26(6), 877-887.

24. Raju J, Roberts J, Taylor M, Patry D, Chomyshyn E, Caldwell D and Mehta R: Toxicological effects of short-term dietary acrylamide exposure in male F344 rats. Environmental toxicology and pharmacology. (2015) 39(1), 85-92.

25. Mahmood SA, Amin KA and Salih SF: Effect of acrylamide on liver and kidneys in albino wistar rats. Int J Curr Microbiol App Sci. (2015) 4(5), 434-44.

26. Atef H, Atteia GM, Rezk HM and El Shafey M: Effect of vitamin E on biochemical ultrastructural changes in acrylamide induced renal toxicity in rats. International Journal of Science Reports. (2017) 3(5), 134-143.

27. Younes A, Autifi MA and Attia H: Protective Effect of N-Acetyl Cysteine in Acrylamide-Induced Hepatotoxicity in Albino Rats. Al-Azhar International Medical Journal. (2020)

28. Hany HO, Atef H, Said E, Elkashef HA and Salem HA: Crocin reverses unilateral renal ischemia reperfusion injury-induced augmentation of oxidative stress and toll like receptor-4 activity. Environmental toxicology and pharmacology. (2018) 59, 182-189.

29. Tsuchida T and Friedman SL: Mechanisms of hepatic stellate cell activation. Nature reviews Gastroenterology & hepatology. (2017) 14(7), 397.

30. Novo E and Parola M: Redox mechanisms in hepatic chronic wound healing and fibrogenesis. Fibrogenesis & tissue repair. (2008) 1(1), 5.

31. De Conti A, Tryndyak V, VonTungeln LS, Churchwell MI, Beland FA, Antunes AM and Pogribny I P: Genotoxic and epigenotoxic alterations in the lung and liver of mice induced by acrylamide: a 28-day drinking water study. Chemical research in toxicology. (2019) 32(5), 869-877.

32. Lee JG, Wang YS and Chou CC: Acrylamide-induced apoptosis in rat primary astrocytes and human astrocytoma cell lines. Toxicology in *Vitro*. (2014) 28(4), 562-570.

33. Zamani E, Shokrzadeh M, Fallah M and Shaki F: A review of acrylamide toxicity and its mechanism. Pharmaceutical and Biomedical Research. (2017) 3(1), 1-7.

34. Chen W, Su H, Xu Y, Bao T and Zheng X: Protective effect of wild raspberry (Rubus hirsutus Thunb.) extract against acrylamide-induced oxidative damage is potentiated after simulated gastrointestinal digestion. Food Chemistry. (2016) 196, 943-952.

35. Ibrahim MA and Ibrahem MD: Acrylamide-induced hematotoxicity, oxidative stress, and DNA damage in liver, kidney, and brain of catfish (Clarias gariepinus). Environmental Toxicology. (2020) 35(2), 300-308.

36. Higashi T, Friedman SL and Hoshida Y: Hepatic stellate cells as key target in liver fibrosis. Advanced drug delivery reviews. (2017) 121, 27–42.Sato Y and Yanagita M: Resident fibroblasts in the kidney: a major driver of fibrosis and inflammation. Inflammation and regeneration. (2017) 37(1), 17.

الملخص العربى

تأثير الانسحاب المفاجئ والتدريجي من مادة الأكريلاميد على الإصابات القشرية الكبدية والكلوية الناتجة عن مادة الأكريلاميد عند ذكور الجرذان البيضاء البالغة: دراسة نسيجية وكيميائية مناعيه

أميرة فتحي أحمد، رندا أحمد إبراهيم، عزة حسين علي، إسراء محمد خيري

قسم الأنسجة وبيولوجيا الخلية، كلية الطب، جامعة المنيا، مصر

الخلفية: تعتبر مادة الأكريلاميد مادة كيميائية صناعية يشيع استخدامها في منتجات عديدة كما أصبحت من أهم اهتمامات الصحة العامة حيث تم اكتشافها في المواد الغذائية المستهلكة على نطاق واسع مثل الخبز المقلي ورقائق البطاطس وأي أطعمة غنية بالكربوهيدرات مطبوخة على درجات حرارة عالية (أعلى من ٢٠٠ درجة مئوية).

الهدف من العمل: دراسة تأثير والسحب المفاجئ والتدريجي لمادة الأكريلاميد على انسجة الكبد و الكلي.

المواد والطرق: تم تنفيذ هذا العمل على ٤٠ من الفئران البيضاء الذكور البالغين. تم تقسيم الفئران إلى ٤ مجموعات، ١٠ جرذان لكل منها: المجموعة الأولى (المجموعة الضابطة). المجموعة الثانية (مجموعة الأكريلاميد): تم اعطاء الفئران الأكريلاميد شفويا عن طريق القناة الهضمية داخل المعدة بجرعة ٢٠ ملغ / كغ مرة واحدة يوميا لمدة ثلاث أسابيع. المجموعة الثالثة (مجموعة الانسحاب المفاجئ): تم اعطاء الفئران الأكريلاميد شفويا عبر طريق القناة الهضمية بجرعة ٢٠ ملغ / كغ مرة واحدة يوميا لمدة ثلاث أسابيع ثم توقف إعطاء الأكريلاميد فجأة في الأسابيع الثلاثة التالية. المجموعة الرابعة (مجموعة الانسحاب التدريجي): تلقوا مادة الأكريلاميد شفويا عبر طريق القناة الهضمية بجرعة ٢٠ ملغ / كغ مرة واحدة يوميا خلال الأسابيع الثلاثة الأولى. في الأسابيع الثلاثة التالية، تم سحب مادة الأكريلاميد تدريجيًا على شكل: ثلاث مرات في الأسبوع الرابع. مرتين في الأسبوع الخامس. مرة واحدة في الأسبوع السادس. ثم تم تحضير الكبد والكلى للدراسات الهستولوجية والهستوكيميائية المناعية والاحصائية.

النتائج: إعطاء مادة الأكريلاميد ادي الي العديد من التغيرات الشكلية في أنسجة الكبد والكلى فى المجموعة الثانية في شكل موت الخلايا المبرمج، واحتقان الأوعية الدموية وتسلل الخلايا الالتهابية. أظهرت المجموعة الثالثة احتفاظا بأنسجة الكبد والكلى إلى حد كبير، بينما أظهرت المجموعة الرابعة تحسنًا طفيفًا. كما أظهرت النتائج انخفاضا ملحوظا في الجليكوجين في معظم خلايا الكبد و الكلي من المجموعة الثانية. فى المجموعة الثالثة كان هناك استعادة لمحتوى الجليكوجين بينما فى المجموعة الرابعة كان هناك تحسنًا طفيفًا. كما كان هناك زيادة في كمية ألياف الكولاجين فى أنسجة الكبد والكلي للمجموعة الثانية. بينما كانت هناك كمية قليلة من ألياف الكولاجين في المجموعة الثالثة. أظهرت المجموعة الرابعة زيادة في كمية ألياف الكولاجين. اما عن النتائج المناعية لوحظ وجود استجابة مناعية كبيرة activated caspase ٣ and alpha smooth muscle actin و انخفاضا في PCNA في أنسجة الكبد و الكلي من المجموعة الثانية. وأظهرت المجموعة الثالثة تحسنًا ملحوظًا على عكس المجموعة الرابعة التي أظهرت تحسنًا طفيفًا.

الخلاصة: يمكن أن نستنتج أن إعطاء مادة الأكريلاميد يسبب العديد من التغيرات الشكلية في أنسجة الكبد والكلى على شكل موت الخلايا المبرمج، واحتقان الأوعية الدموية، والتسلل الخلوي الالتهابي. عند الانسحاب المفاجئ لمادة الأكريلاميد، حدث تحسن ملحوظ. بينما أدى الانسحاب التدريجي لمادة الأكريلاميد إلى تحسنًا طفيفًا.